Development of an Isobaric Transfer Viscometer Operating up to 140 MPa. Application to a Methane + Decane System

Pierre Daugé, Antoine Baylaucq, Laurent Marlin, and Christian Boned*

Laboratoire des Fluides Complexes, Faculté des Sciences, BP 1155, 64013 Pau Cedex, France

A falling body viscometer with electromagnetic detection and operating at pressures up to 140 MPa and temperatures up to 120 °C has been developed in order to measure the dynamic viscosity of fluids with a low viscosity (i.e. methane) and which are not single phase at normal pressure. The isobaric transfer procedure from an additional cell to the measuring cell is described. The calibration procedure is also explained, and the measurements on the binary methane + decane ($x_{\text{methane}} = 0.3124$) are presented (65 experimental data).

1. Introduction

The dynamic viscosity η of fluid mixtures is of great interest in various research areas, both applied and fundamental. A large number of studies have been performed on the variation of η with temperature, composition, and chemical species of the components, but most of the studies have been carried out at normal pressure. Studies as a function of pressure are much less frequent. In this laboratory[1−3] the dynamic viscosities of various pure substances and mixtures have been studied as a function of temperature, composition, and pressure, studies closely related to petroleum engineering problems. Fluids involved in such areas are particularly complex, especially those containing light alkanes, such as methane, which are monophasic at high pressures (at bottom well conditions) and polyphasic at normal pressure. The viscometer available at the laboratory[4] to date could only be filled at atmospheric pressure, which required the sample to be in the liquid state. This apparatus allows only the study, for petroleum engineering, of oils[5] free of gas.

We have designed a new viscometer which can be filled at high pressure following an isobaric procedure. Consequently, the study of the dynamic viscosity of samples containing a high proportion of light hydrocarbons is now possible. Usually such fluids have a very low viscosity and the design of the apparatus took also into account this specificity of the samples.

2. Isobaric Transfer System

Apparatus. The filling technique of the viscometer is based on an isobaric transfer procedure at high pressure. To ensure a correct transfer, the temperature and pressure conditions have to be chosen so that the fluid is in a monophasic liquid state. This is compulsory in order to have the same fluid in the apparatus as in the pressurized reservoir cell containing the sample. According to the volume of the measurement cell (about 20 cm^3), a volume of 120 cm^3 of sample is necessary for the complete procedure described hereafter. The system, which is shown in Figure 1, is composed of two high-pressure piston cells called "cell 1" and "cell 2" (TOP Industrie) of unit volume 120 cm^3 and operating up to 150 MPa, a gas compressor (NOVA Swiss) capable of pressures up to 300 MPa (but 100 MPa is enough for the transfer procedure), the reservoir cell which contains the pressurized sample, a vacuum pump (LEYBOLD, TRIVAC Type), and an electrically controlled double-chamber displacement pump (ROP), of maximum pressure 60 MPa. Both chambers of this pump contain a compression oil instead of mercury, which was often used in high-pressure techniques. The valves are of AUTOCLAVE and SITEC types.

Preliminary Steps. The first task is to bring the reservoir to the temperature and pressure conditions for which the sample is a liquid single-phase. It is generally necessary to increase the pressure and sometimes the temperature in the reservoir. During pressure increase it is essential to agitate the reservoir in order to preserve the homogeneity of the sample. Let us assume then that the sample is in the reservoir at pressure P_2 and at a temperature such that the sample is multiphase. Pump chamber 2, which is at pressure $P_1 > P_2$, is connected to the reservoir so that an intermediate pressure P_3 is reached at equilibrium. To raise the pressure P of the sample beyond the bubble pressure (for the temperature T considered), the reservoir is filled with compression oil. The volume introduced is monitored (120 cm^3 of sample at the required (P, T) conditions are necessary to perform the measurements).

Cells 1 and 2 have then to have their piston placed at an end and be fully filled with compression oil raised to pressure P corresponding to the pressure required for the future transfer. The entire transfer will then be processed following two stages: first a transfer from the reservoir to cell 1 and then a transfer from cell 1 to the viscometer proper. To achieve these two transfers, the double-chamber pump must be used; the pump's electric control allows chambers 1 and 2 to be used either independently or simultaneously.

Transfer from the Reservoir Cell to Supplementary Cell 1. This first part of the transfer consists of moving 120 cm^3 of the sample from the reservoir to cell 1 at constant pressure P. The reservoir and cell 1 are isolated from the rest of the apparatus, and compression oil is introduced in the reservoir with pump chamber 2, while pump chamber 1 is filled up with compression oil, the entire

* To whom correspondence should be addressed. Fax: (+33) 559 80 83 82. E-mail: christian.boned@univ-pau.fr.

10.1021/je000371v CCC: $20.00
Published on Web 05/15/2001

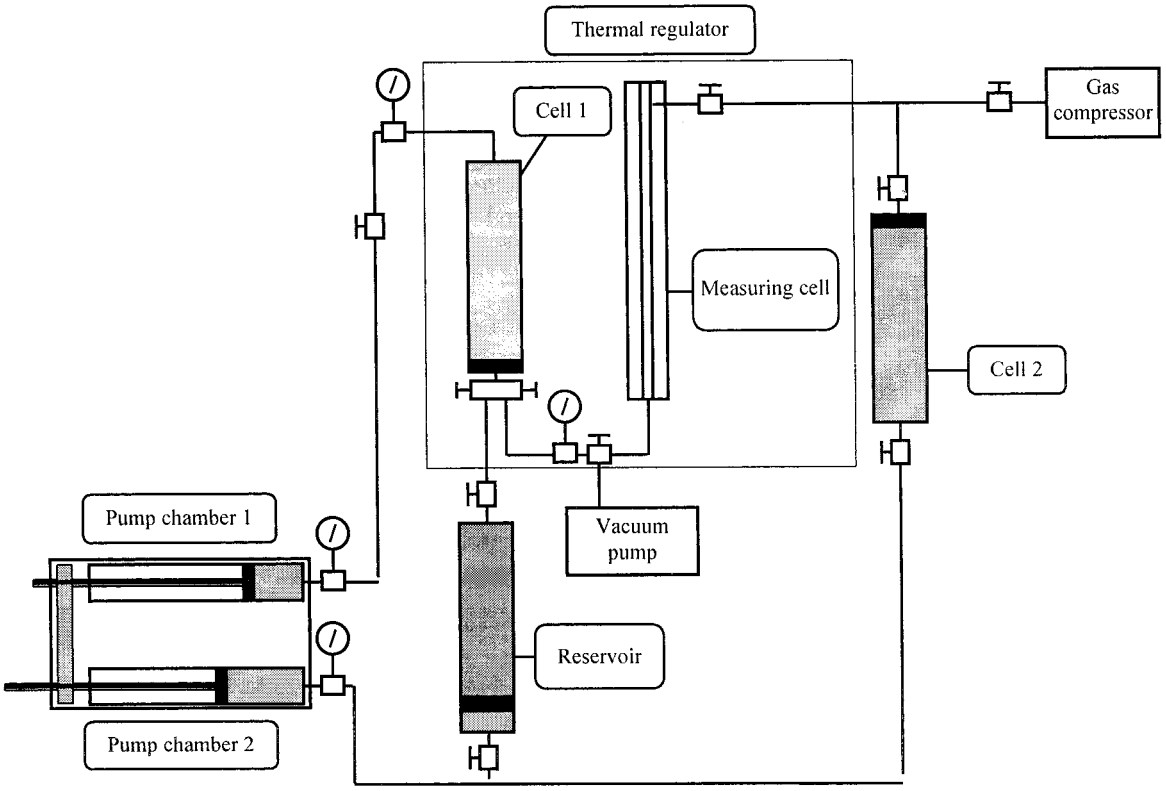

Figure 1. Description of the device.

operation being carried out at constant pressure P. The transfer is stopped when ~120 cm^3 of the fluid is located in cell 1.

At this stage the reservoir is removed, and the part between the cells (1 and 2) including the measuring cell is brought to pressure P using the gas compressor (with helium for example).

Filling the Measuring Cell. Cell 1 is connected to the measuring cell (full of compressed gas) and cell 2 (full of compression oil). The sample fluid contained in cell 1 and the gas are evacuated as rapidly as possible toward cell 2 by means of the double-chamber pump. Cell 2 recovers the gas and a part of the sample fluid which may have been polluted during the transfer. In all, the equivalent of 3 times the volume of the measuring cell is transferred (i.e. 60 cm^3) in order to ensure that the sample within it (20 cm^3 in all) is unpolluted. Cell 2, the double-chamber pump, and the gas compressor are removed.

Changing Pressure. The double-chamber pump is removed and replaced by a NOVA-brand pneumatic pump, with a maximum pressure of 160 MPa, which is connected to cell 1. It is thus possible to perform investigations up to 150 MPa with no difficulty. As for temperature, the experiments are performed within the temperature interval 0 °C to 120 °C. The latter limit value is a constraint imposed by the specifications of the various elements used in the assembly, in particular the pressure gauge connections, whose capabilities are not guaranteed at temperatures higher than 120 °C. Pressure is varied by simply adding or removing compression oil from cell 1. Pressure is monitored by means of a pressure gauge (HBM-P3M type), which can measure pressures up to 200 MPa, connected directly to the capillary tube between the measuring cell and cell 1. This allows us to measure the real pressure of the sample. It is accurate to within ±0.2 MPa.

3. Falling Body Viscometer

Principle of the Viscometer. In this type of viscometer, a cylindrical sinker with hemispherical ends falls vertically in the fluid studied along the symmetrical axis of the device. The fluid is forced to flow through the annulus between the sinker and the tube. Studying the falling body[6] reveals that measurement of the terminal velocity can be used to determine the viscosity $\eta(P,T)$ of the fluid. The time $\Delta\tau$ of the fall between two fixed reference points is measured, and the viscosity η of the fluid is often calculated using the following equation:

$$\eta = K(\rho_S - \rho_L)\Delta\tau \quad (1)$$

ρ_S is the equivalent density of the falling body (which may be hollow or composite), ρ_L is that of the fluid, and K is a quantity characteristic of the viscometer and of the falling body. However, for the fluids with a low viscosity, negative effects appear and various authors[7−12] have indicated another form: $\eta = f(\Delta\tau\Delta\rho)$ with $\Delta\rho = \rho_S - \rho_L$. The following form can be used:

$$\eta = a(\Delta\tau\Delta\rho)^2 + b(\Delta\tau\Delta\rho) + c \quad (2)$$

in which parameters a, b, and c are determined by calibration[13] with three well-known fluids in the (P, T) range. Other types of equations can be considered, but in any case, it is unwise to use the extrapolation part below the lowest calibration viscosity (methane in our case). The density measurements are performed by means of a semiautomatic Anton Paar DMA 60 densimeter equipped with its high pressure 512P cell, which allows measurements up to 70 MPa with an accuracy of about 0.1 kg·m^{-3}. Data were then estimated up to 140 MPa with a Tait-like equation with an accuracy on the order of that of an equation of state (see Table 1 and section 5).

Table 1. Measured and Estimated Densities and Viscosities of the Mixture Methane (1) + Decane (2) ($x_1 = 0.3124$)

P	ρ_{exp}[a]	ρ_{EOS}[b]		η_{exp}[c]	η_{EOS}[d]	
MPa	g·cm^{-3}	g·cm^{-3}	$1-\rho_{EOS}/\rho_{exp}$	mPa·s	mPa·s	$1-\eta_{EOS}/\eta_{exp}$
			T/°C = 20			
20	0.7004	0.7103	−1.41%	0.6376	0.6358	0.28%
30	0.7078	0.7169	−1.28%	0.6996	0.6977	0.27%
40	0.7145	0.7231	−1.20%	0.7650	0.7631	0.25%
50	0.7207	0.7288	−1.13%	0.8341	0.8321	0.24%
60	0.7265	0.7343	−1.08%	0.9070	0.9050	0.22%
70	0.7318	0.7394	−1.05%	0.9839	0.9818	0.21%
80	0.7368	0.7444	−1.03%	1.0651	1.0629	0.21%
90	0.7415	0.7491	−1.02%	1.1509	1.1485	0.21%
100	0.7459	0.7535	−1.02%	1.2414	1.2388	0.21%
110	0.7502	0.7579	−1.03%	1.3370	1.3341	0.22%
120	0.7542	0.7620	−1.04%	1.4378	1.4347	0.22%
130	0.7580	0.7660	−1.05%	1.5443	1.5409	0.22%
140	0.7617	0.7699	−1.07%	1.6566	1.6529	0.22%
			T/°C = 40			
20	0.6853	0.6963	−1.60%	0.4962	0.4944	0.36%
30	0.6936	0.7035	−1.42%	0.5435	0.5418	0.31%
40	0.7010	0.7101	−1.30%	0.5936	0.5919	0.29%
50	0.7077	0.7163	−1.21%	0.6465	0.6448	0.26%
60	0.7138	0.7221	−1.16%	0.7025	0.7008	0.24%
70	0.7194	0.7276	−1.13%	0.7618	0.7599	0.25%
80	0.7247	0.7327	−1.12%	0.8244	0.8224	0.24%
90	0.7295	0.7377	−1.12%	0.8907	0.8885	0.25%
100	0.7341	0.7424	−1.13%	0.9607	0.9583	0.25%
110	0.7384	0.7469	−1.15%	1.0347	1.0322	0.24%
120	0.7425	0.7512	−1.17%	1.1130	1.1102	0.25%
130	0.7464	0.7554	−1.20%	1.1957	1.1926	0.26%
140	0.7501	0.7594	−1.24%	1.2831	1.2797	0.26%
			T/°C = 60			
20	0.6701	0.6821	−1.78%	0.4104	0.4087	0.41%
30	0.6793	0.6899	−1.56%	0.4404	0.4388	0.36%
40	0.6874	0.6970	−1.39%	0.4753	0.4738	0.32%
50	0.6948	0.7036	−1.27%	0.5144	0.5129	0.29%
60	0.7016	0.7097	−1.16%	0.5572	0.5557	0.27%
70	0.7078	0.7155	−1.09%	0.6031	0.6016	0.25%
80	0.7136	0.7210	−1.03%	0.6521	0.6505	0.25%
90	0.7191	0.7262	−0.99%	0.7037	0.7022	0.21%
100	0.7242	0.7311	−0.95%	0.7579	0.7563	0.21%
110	0.7290	0.7358	−0.93%	0.8145	0.8128	0.21%
120	0.7336	0.7403	−0.92%	0.8733	0.8716	0.19%
130	0.7380	0.7447	−0.91%	0.9343	0.9324	0.20%
140	0.7421	0.7488	−0.90%	0.9973	0.9953	0.20%
			T/°C = 80			
20	0.6551	0.6676	−1.91%	0.3553	0.3537	0.45%
30	0.6653	0.6761	−1.62%	0.3786	0.3772	0.37%
40	0.6746	0.6838	−1.36%	0.4057	0.4044	0.32%
50	0.6825	0.6908	−1.21%	0.4362	0.4350	0.28%
60	0.6896	0.6974	−1.12%	0.4695	0.4683	0.26%
70	0.6961	0.7035	−1.07%	0.5054	0.5042	0.24%
80	0.7020	0.7093	−1.03%	0.5437	0.5424	0.24%
90	0.7075	0.7147	−1.01%	0.5840	0.5827	0.22%
100	0.7126	0.7198	−1.01%	0.6264	0.6249	0.24%
110	0.7174	0.7248	−1.03%	0.6706	0.6690	0.24%
120	0.7219	0.7295	−1.05%	0.7166	0.7149	0.24%
130	0.7262	0.7340	−1.07%	0.7642	0.7624	0.24%
140	0.7302	0.7383	−1.10%	0.8135	0.8115	0.25%
			T/°C = 100			
20	0.6427	0.6531	−1.62%	0.2975	0.2963	0.40%
30	0.6542	0.6623	−1.24%	0.3168	0.3158	0.32%
40	0.6640	0.6706	−0.99%	0.3392	0.3384	0.24%
50	0.6729	0.6781	−0.78%	0.3642	0.3636	0.16%
60	0.6807	0.6851	−0.65%	0.3916	0.3909	0.18%
70	0.6879	0.6916	−0.53%	0.4209	0.4203	0.14%
80	0.6945	0.6976	−0.45%	0.4520	0.4515	0.11%
90	0.7006	0.7033	−0.39%	0.4848	0.4843	0.10%
100	0.7062	0.7087	−0.35%	0.5191	0.5187	0.08%
110	0.7116	0.7138	−0.32%	0.5549	0.5545	0.07%
120	0.7166	0.7187	−0.29%	0.5921	0.5917	0.07%
130	0.7214	0.7234	−0.28%	0.6305	0.6301	0.06%
140	0.7259	0.7279	−0.27%	0.6702	0.6698	0.06%

[a] ρ_{exp} = Anton Paar 512P (P < 70 MPa) + extrapolation ($P \leq$ 140 MPa). [b] ρ_{EOS} = Lee Kesler EOS + Spencer and Danner mixing law. [c] η_{exp} = viscosity estimated using ρ_{exp}. [d] η_{EOS} = viscosity estimated using ρ_{eos}.

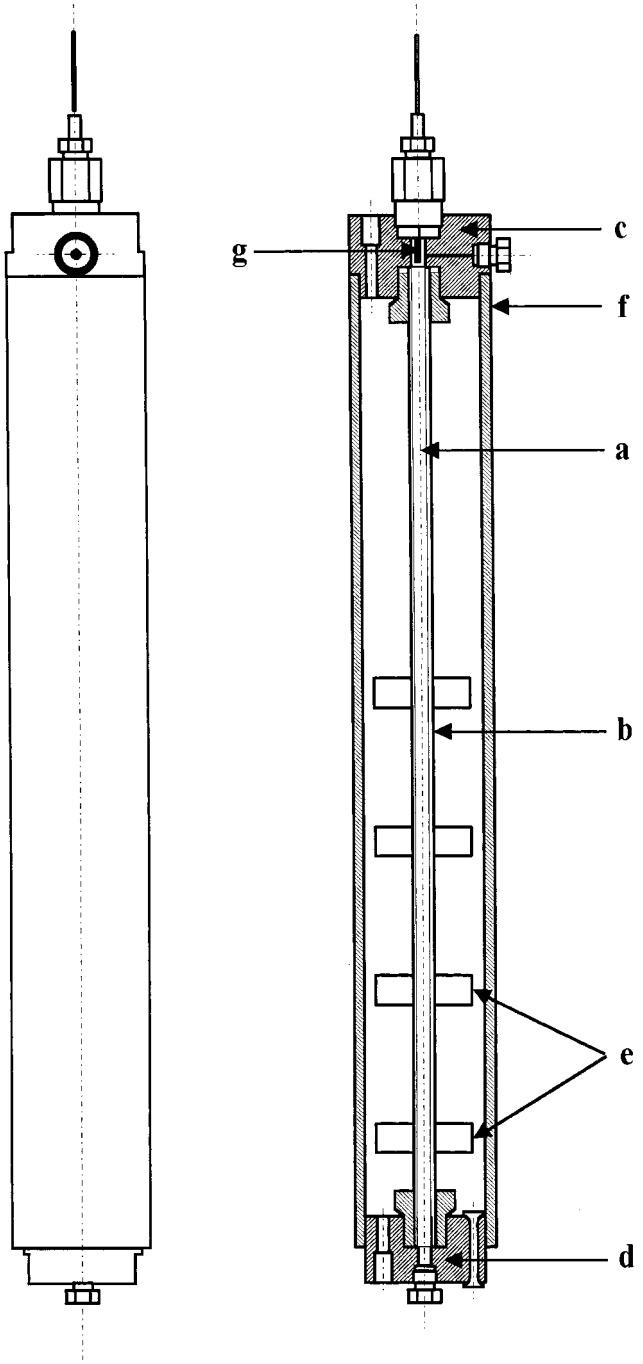

Figure 2. Schematic description of the measuring cell.

Description of the Measuring Cell. The measuring block is represented schematically in Figure 2, which shows two sections. It is made up of a cylindrical tube b (internal diameter 8 mm, external diameter 14.3 mm, length 600 mm, maximum pressure allowed 200 MPa), which contains an inner cylindrical tube a (internal diameter 6.47 mm, external diameter 7.94 mm, length 600 mm) ended up with two HP connectors c and d. The sample is filled in both tubes. Four holes are drilled on the inner tube in order to have the same pressure inside and outside the inner tube and then avoid any deformation of the inner tube itself. Four electrical coils e are fitted on the outer tube in order to detect the passage of the falling body; a variation of the magnetic flux is detected through the coils. The space allowed between the HP tube a and the aluminum cylinder f contains a heat-carrying liquid which is used to thermoregulate the whole system. Temperature maintenance is

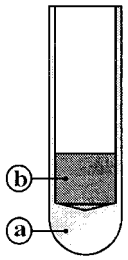

Figure 3. Description of the falling body: (a) aluminum body; (b) magnetic core.

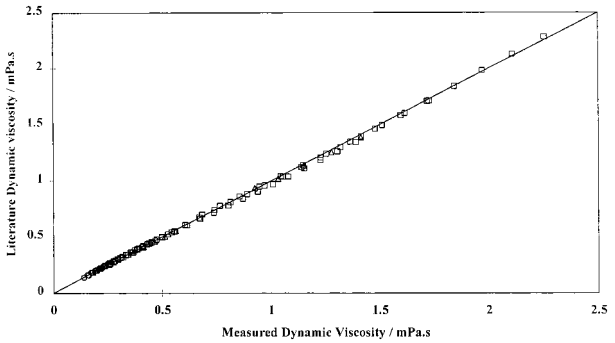

Figure 4. Comparison of the measured and literature viscosities of pentane and decane, $\eta_{LIT} = f(\eta_{exp})$: ○, Kiran and Sen;[10] □, Oliveira and Wakeham;[18] △, Knapstad et al.[23]

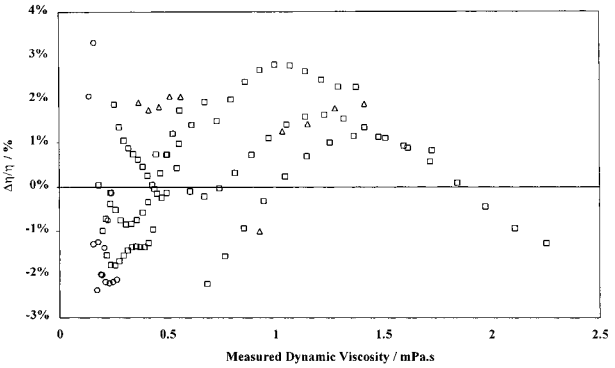

Figure 5. Deviations of the literature dynamic viscosity of pentane and decane as a function of the measured data: O, Kiran and Sen;[10] □, Oliveira and Wakeham;[18] △, Knapstad et al.[23]

controlled by an AOIP system in which the MESUREX probe is placed inside the cell through the aperture g. The heat-carrying circuit is connected to a thermostat (HUBER brand, UNISTAT model) whose thermostatic bath can be regulated to within 0.05 °C in the temperature range −30 °C to +200 °C. Pressure in the measuring cell is obtained by means of a supplementary cell (cell 1 in Figure 1) fitted with a piston, also filled with sample fluid, and which is kept in communication with the measuring cell. The compression liquid is kept on the other side of its piston, which avoids direct contact between the fluid studied and the compression liquid. Both measuring and piston cells are placed in an automated air-pulsed thermal regulator in order to get an homogeneous temperature in the manifold.

Detection System. It is based on an electromagnetic effect induced by the sinker passing through the coils (four pairs wound from insulated copper wire) located on the tube, as shown in Figure 2. Each pair of coils consists of a "primary" and a "secondary" coil; the four secondary coils are connected in series while the four primary ones are connected in parallel to a variable-frequency generator,

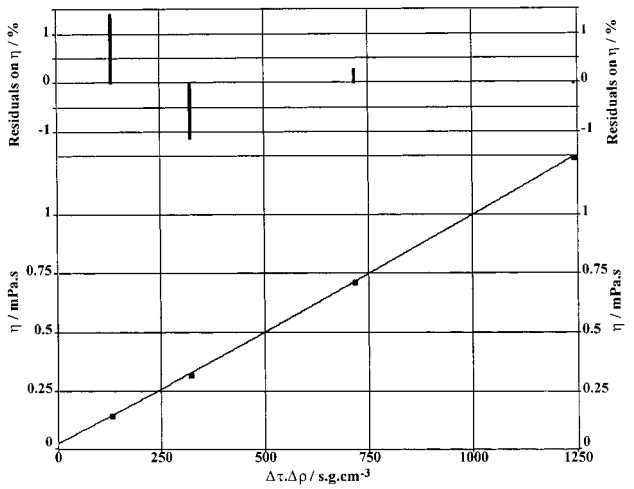

Figure 6. Calibration curve at $t = 40$ °C and $P = 60$ MPa (—, eq 2) along with the residuals (%).

providing an input signal on the order of 10 V and 1000 Hz.

A hollow aluminum sinker (a in Figure 3), with a magnetic core (b) glued with Araldite inside of it, was constructed with an outside diameter of 6.35 mm, an inside diameter of 5 mm, and a length of 20 mm (the ratio of the weight diameter to the tube diameter is 0.98, substantially above the value of 0.93 to minimize eccentricity effects[11,14]). Its apparent density is $\rho_S = 4650$ kg·m^{-3}.

When the sinker passes through the first pair of coils, the inductance of the coil increases and the secondary circuit is unbalanced and is used to operate a trigger which starts an electronic timer. The next three pairs of coils switch off the timer in a similar manner so that three fall times for the same temperature and pressure conditions are measured. The comparison of these three fall times shows that the maximum fall velocity is reached before the very first coil. The length of the tube (600 mm) ensures that the distance ran by the sinker before it reaches the first coils is long enough to have ended the acceleration motion of the fall. The system with four coils is an important caution because this system aims at measuring low dynamic viscosity and thus shorter fall times.

Cell 1 and the measuring cell are able to rotate through 180° about the horizontal axis, so that a set of measurements can be processed under the same temperature and pressure conditions.

4. Calibration Procedure

Calibration for Viscous Fluids (η > 0.1 mPa·s). This procedure is used in order to determine the parameter K, which is introduced in eq 1. Toluene has been taken as a reference fluid, as a large number of data are available in our experimental temperature and pressure ranges, both for viscosity and density. Literature data[15−21] have been used in order to evaluate $K(P,T)$ for each P, T set. It is important to notice here that the density of toluene (ρ_L) is about 850 kg·m^{-3} in our experimental range. An error of 10 kg·m^{-3} on ρ_L (about 1%), which is a large error, leads to a relative error of about 1/400 on η (0.25%).

After calibration with toluene, measurements have been carried out on pentane and decane, for which data are available in the literature.[10,16,18,22,23] The comparison of our data with those from the literature shows a relative deviation ($\Delta\eta/\eta$) lower than 2.5%, which is around the experimental uncertainty of such high-pressure viscometers. During those experiments, the lowest measured

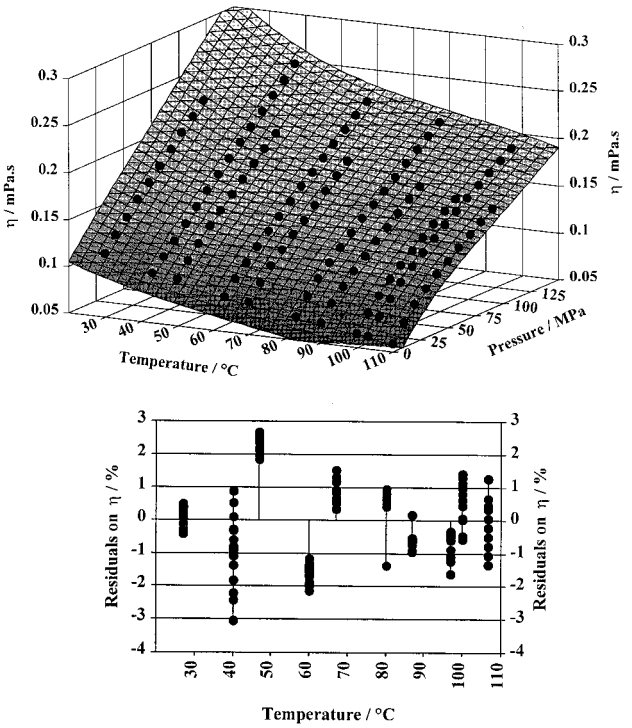

Figure 7. Dynamic viscosity (a) and residuals (b) of propane as a function of T and P. Comparison with data of Vogel and Küchenmeister.[26]

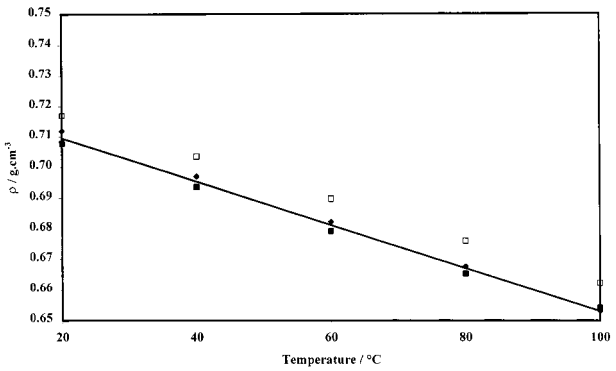

Figure 8. Binary mixture methane (1) + decane (2) ($x_1 = 0.3124$). Variations of density as a function of temperature at $P = 30$ MPa: □, equation of state; ◆, Knapstad et al.;[28] ■, this work.

viscosity is of pentane at 100 °C and 10 MPa, which is 0.137 mPa·s. Figure 4 shows the good agreement of our data for pentane and decane with those from the literature (0.137 < η < 2.28 mPa·s). The curve $\eta_{lit.} = f(\eta_{meas})$ is almost the first bisectrix. Figure 5 displays, under the same conditions, the deviation between pentane and decane literature data and our data.

Calibration for Fluids with Low Viscosity. In this case it is better to use eq 2. For the calibration, measurements have been done on toluene, pentane, carbon dioxide,[24] and methane.[25] For each P, T set, the curve $\eta = f(\Delta\tau\Delta\rho)$ is plotted. For example, Figure 6 shows this curve at $t = 40$ °C and $P = 60$ MPa ($\Delta\tau$ is taken between coils 1 and 4). A slight curvature can be observed for the low-viscosity data but which has to be taken into account. The line represents the curve of eq 2. The calibration has then been used to determine the viscosity of propane, which has been tested against literature data.[26,27] Vogel and Küchenmeister[26] give viscosity data at pressures higher than 40 MPa with a relative error $\Delta\eta/\eta$ of 4%. Figure 7 displays our experimental data on propane along with those from

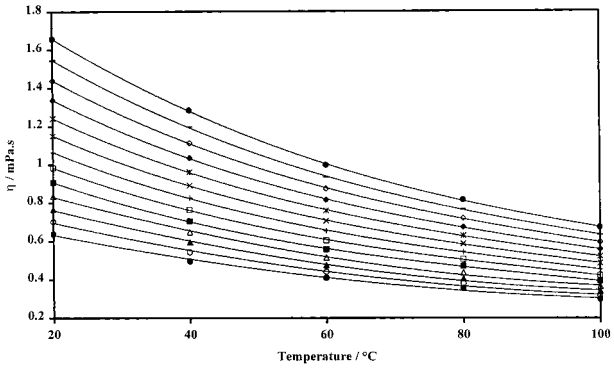

Figure 9. Binary mixture methane (1) + decane (2) ($x_1 = 0.3124$). Variations of dynamic viscosity η_{EXP} as a function of temperature for various pressures: ●, 20 MPa; ○, 30 MPa; ▲, 40 MPa; △, 50 MPa; ■, 60 MPa; □, 70 MPa; +, 80 MPa; ×, 90 MPa; ∗, 100 MPa; ◆, 110 MPa; ◇, 120 MPa; —, 130 MPa; ●, 140 MPa.

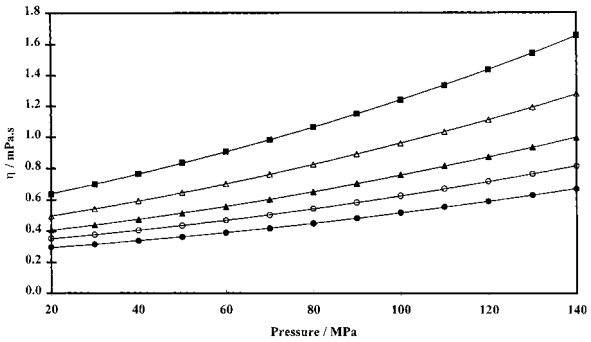

Figure 10. Binary mixture methane (1) + decane (2) ($x_1 = 0.3124$). Variations of dynamic viscosity η_{EXP} as a function of pressure for various temperatures: ■, 20 °C; △, 40 °C; ▲, 60 °C; ○, 80 °C; ●, 100 °C.

the literature, at $t = 40$ °C as a function of pressure. The agreement is very good up to 100 MPa, as the deviation is around 3%. For pressures above 100 MPa no data were available in the literature cited.

5. Application to the Methane + Decane Binary Mixture

Presentation. The methane + decane system has already been studied[28] but at pressures lower than 41 MPa (9.78 MPa ≤ P ≤ 40.92 MPa) and in the temperature range 19.1 °C ≤ t ≤ 157.6 °C. To achieve the development of our apparatus, we decided to choose a methane + decane mixture at a given composition, as a test fluid, which has been studied.[28] The one we studied contains methane with a molar fraction of 0.3124 (mass fraction of 0.0487). It must be stressed here that Knapstad et al.[28] have used a completely different technique in order to determine the viscosity of the system considered. They used an oscillating cup viscometer. The methane used in our mixture is from Rectapur with a purity greater than 99.9%, and the decane is from Sigma with a purity of 99.4%. The phase diagram[29] of the methane + decane system shows that the mixture we chose is always in a monophasic liquid state at pressures higher than 15 MPa (at temperatures lower than 104.4 °C). The transfer of the sample has been carried out at a higher pressure ($P \approx 40$ MPa).

Density Measurements. The values of density ρ_L up to 70 MPa have been determined by means of an Anton Paar DMA60+DMA601 resonator densimeter, equipped with a 512P high-pressure cell. These experimental data have been extrapolated for each temperature up to 140 MPa,

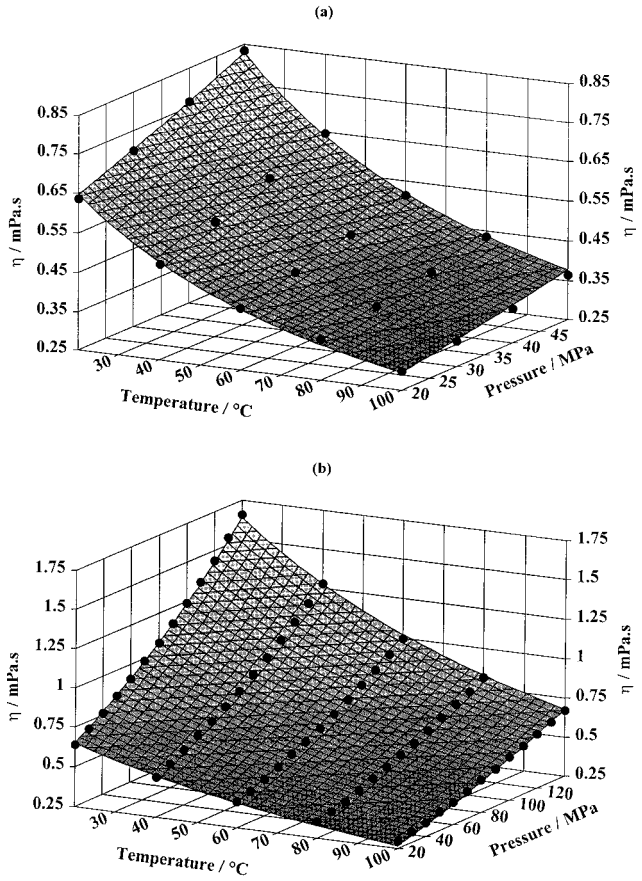

Figure 11. Binary mixture methane (1) + decane (2) (x_1 = 0.3124). Surface $\eta_{exp}(P,T)$: (a) pressure up to P = 50 MPa; (b) pressure up to P = 140 MPa.

following the procedure described by Et-Tahir et al.[3] and using a Tait-like equation. The uncertainty on ρ_L is lower than 0.1 kg·m^{-3}, which is on the order of the estimation made by other authors[9] who used the same type of equipment. The data obtained are displayed in Table 1 (column ρ_{exp}). Measured and extrapolated density values have been compared with the one generated by the Lee and Kesler equation of state,[30] using methane and decane as reference substances.[31] For the calculation of the "pseudo-critical" coordinates, the Spencer and Danner[32] mixing rule has been applied. The data then obtained are displayed in Table 1 in column ρ_{EOS}. It can be noticed that $\rho_{EOS} > \rho_{exp}$, that the average deviation is around 1%, and that the maximum deviation is 1.91%. Figure 8 displays the variations of density as a function of temperature, at P = 30 MPa, including the data generated by the equation of state and the interpolated data of Knapstad. The solid line represents the best curve calculated from the two sets of experimental data; a good agreement between these two sets can be observed.

Dynamic Viscosity Measurements. The measurements have been carried out at T = (293.15, 313.15, 333.15, 353.15, and 373.15) K and P = (20, 30, 40, 50, 60, 70, 80, 90, 100, 110, 120, 130, and 140) MPa, which represent 65 (P, T) sets. In Table 1 column η_{exp} displays the values obtained using ρ_{exp} in the $\Delta\rho$ term, whereas column η_{EOS} displays the values obtained using ρ_{EOS} in the same term. Table 1 also provides the values of $(1 - \eta_{EOS}/\eta_{exp})$. The absolute average deviation is 0.24%, and the maximum deviation is 0.45%. These results confirm the previous remark about the influence of ρ_L: an error of 1% on ρ_L leads to an error of 0.25% on η. For P < 70 MPa, ρ_{EOS} is always above ρ_{exp}, which is experimentally determined. Above this pressure, the density estimated with the Tait equation is still below ρ_{EOS}, with similar deviations. We think that the results for viscosity are more accurately determined with extrapolated density than with ρ_{EOS}. Figure 9 displays the variations of η_{exp} as a function of temperature for various pressures, and Figure 10 shows the variations of η_{exp} as a function of pressure for various temperatures. Parts a and b of Figure 11 show the surfaces $\eta_{exp}(P,T)$, the first one for pressures up to 50 MPa and the second one up to 140 MPa.

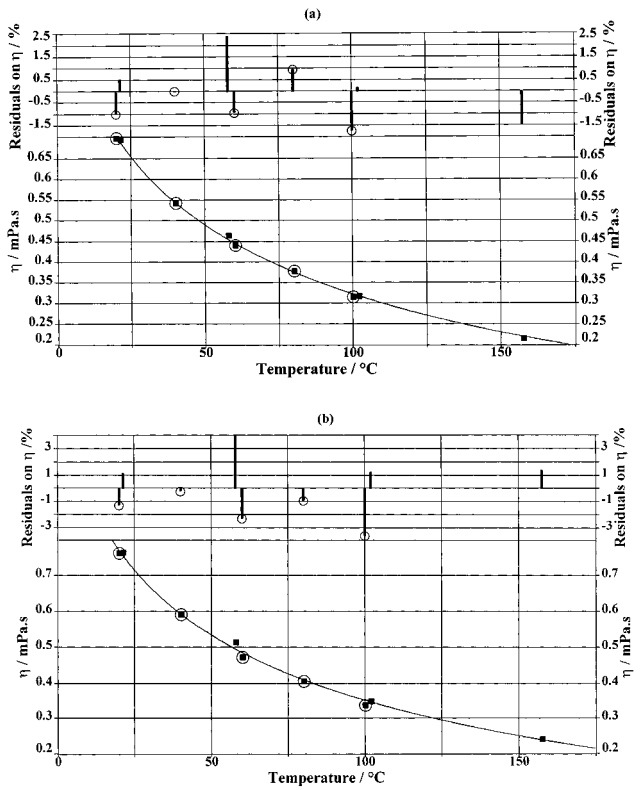

Figure 12. Binary mixture methane (1) + decane (2) (x_1 = 0.3124). Comparison of our viscosity data (⊙) and those from Knapstad et al.[28] (●): (a) P = 30 MPa; (b) P = 40 MPa.

Our experimental data have been compared with those given by Knapstad et al.[28] on the same mixture. Figure 12 displays the variations of η at P = 30 MPa and P = 40 MPa as a function of temperature. A very good agreement between our data and those of Knapstad et al.[28] can be observed. The solid line represents the best curve from which the deviations are calculated. It must be noticed that Knapstad values are not given exactly at 30 and 40 MPa; for example, they give data at 40.56 MPa at 21.31 °C, 40.92 MPa at 58.04 °C, 39.89 MPa at 102 °C, 41.95 MPa at 157.6 °C, 29.88 MPa at 21.33 °C, 29.8 MPa at 57.82 °C, 30.06 MPa at 101.9 °C, and 30.04 MPa at 157.4 °C. To have a correct comparison accounting for the exact values of the authors, the surface $\eta(P,T)$ has been plotted with our values and Knapstad values. Figure 13 displays the surface then obtained along with the deviations; the temperature range corresponds to our experimental range (20, 40, 60, 80, and 100 °C). Figure 14 displays the same surface with no limitation in temperature; the agreement is still correct enough. The uncertainty indicated by Knapstad varies from ±1% at 20 °C to ±2.5% at 160 °C. For our apparatus, according to the various comparisons and tests we have made on fluids with either low or high viscosity, the estimated uncertainty up to 140 MPa can be around 3%.

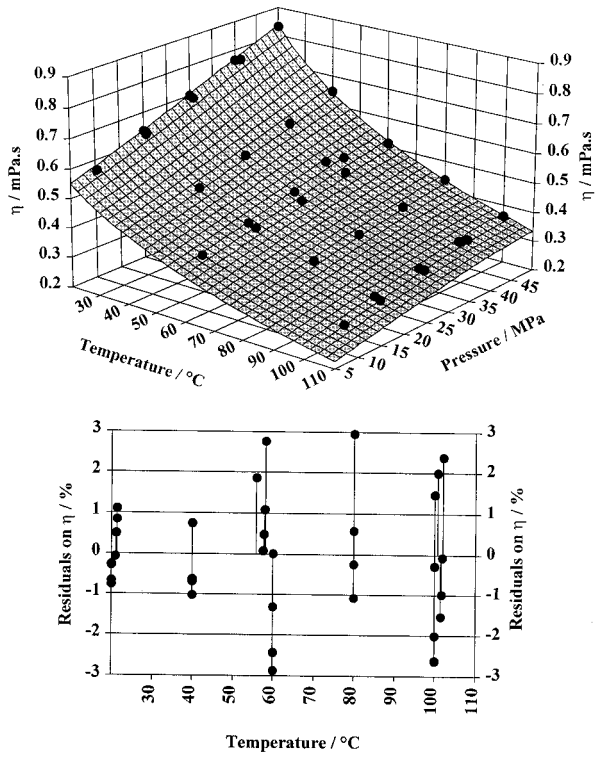

Figure 13. Binary mixture methane (1) + decane (2) (x_1 = 0.3124). Surface $\eta(P,T)$ displaying our viscosity data and those from Knapstad et al.[28] ($t \leq 100$ °C).

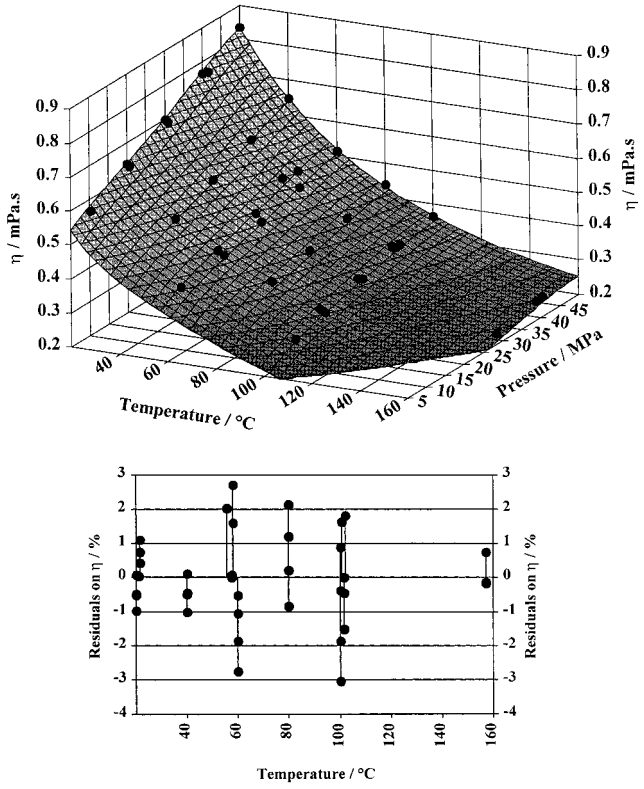

Figure 14. Binary mixture methane (1) + decane (2) (x_1 = 0.3124). Surface $\eta(P,T)$ displaying our viscosity data and those from Knapstad et al.[28] ($t \leq 160$ °C).

6. Conclusion

The development of a new falling body viscometer operating at pressures up to 140 MPa and temperatures up to 120 °C has been presented. The main feature of this device is the ability to study the viscosities of samples which are not single phase at atmospheric pressure.

The application to the binary system methane + decane has been presented and compared to previous measurements done on another type of viscometer, and good agreement has been shown. The estimation of the precision of this new device is better than 3%.

Literature Cited

(1) Boned, C.; Moha-Ouchane, M.; Allal, A.; Benseddik, M. Viscosity and Density at High Pressures in an Associative Ternary. *Int. J. Thermophys.* **1998**, *19*, 1325−1341.
(2) Baylaucq, A.; Daugé, P.; Boned, C. Viscosity and Density of the Ternary System Heptane + Methylcylohexane + 1-Methylnaphthalene. *Int. J. Thermophys.* **1997**, *18*, 1089−1107.
(3) Et-Tahir, A.; Boned, C.; Lagourette, B.; Xans, P. Determination of the Viscosity of Various Hydrocarbons and Mixtures of Hydrocarbons Versus Temperature and Pressure. *Int. J. Thermophys.* **1995**, *16*, 1309−1334.
(4) Ducoulombier, D.; Lazarre, F.; Saint-Guirons, H.; Xans, P. Viscosimètre à Corps Chutant Permettant de Procéder à des Mesures de Viscosité de Liquides sous Hautes Pressions. *Rev. Phys. Appl.* **1985**, *20*, 735−740.
(5) Kanti, M.; Zhou, H.; Ye, S.; Boned, C.; Lagourette, B.; Saint-Guirons, H.; Xans, P.; Montel, F. Viscosity of Liquid Hydrocarbons, Mixtures and Petroleum Cuts, as a Function of Pressure and Temperature. *J. Phys. Chem.* **1989**, *93*, 3860−3864.
(6) Borisov, V. B. The Equation for a Falling-Cylinder Viscometer. *High Temp.* **1998**, 36, 293−298.
(7) Irving, J. B.; Barlow, A. J. An Automatic High-Pressure Viscometer *J. Phys. E: Sci. Instrum.* **1971**, *4*, 232−236.
(8) Isdale, J. D.; Spence, C. M. A Self-Centring Falling Body Viscometer for High Pressures. National Engineering Laboratory, Report No. 592, 1975.
(9) Papaioannou, D.; Bridakis, M.; Panayiotou, G. Excess Dynamic Viscosity and Excess Volume of *N*-Butylamine + 1-Alkanol Mixtures at Moderately High Pressure *J. Chem. Eng. Data* **1993**, *38*, 370−378.
(10) Kiran, E.; Sen, Y. L. High-Pressure Viscosity and Density of *n*-Alkanes. *Int. J. Thermophys.* **1992**, *13*, 411−442.
(11) Sen, Y. L.; Kiran, E. A New Experimental System to Study the Temperature and Pressure Dependence of Viscosity, Density, and Phase Behavior of Pure Fluids and Solutions. *J. Supercrit. Fluids* **1990**, *3*, 91−92.
(12) Tilly, K. A.; Foster, N. R.; Macnaughton, S. J.; Tomasko, D. L. Viscosity Correlations for Binary Supercritical Fluids. *Ind. Eng. Chem. Res.* **1994**, *33*, 681−688.
(13) Kiran, E.; Gokmenoglu, Z. High-Pressure Viscosity and Density of *n*-Alkanes. *J. Appl. Polym. Sci.* **1995**, *58*, 2307−2324.
(14) Chen, M. C. S.; Lescarboura, J. A.; Swift, G. W. The Effect of Eccentricity on the Terminal Velocity of the Cylinder in a Falling Cylinder Viscometer. *AIChE J.* **1968**, *14*, 123−127.
(15) Kashiwagi, H.; Hashimoto, T.; Tanaka, Y.; Kubota, H.; Makita, T. Thermal Conductivity and Density of Toluene in the Temperature Range 273−373 K at Pressures up to 250 MPa. *Int. J. Thermophys.* **1982**, *3*, 201−215.
(16) Kashiwagi, H.; Makita, T. Viscosity of Twelve Hydrocarbon Liquids in the Temperature Range 298−348 K at Pressures up to 110 MPa. *Int. J. Thermophys.* **1982**, *3*, 289−305.
(17) Krall, A. H.; Sengers, J. V.; Kestin, J. Viscosity of Liquid Toluene at Temperatures from 25 to 150 °C and at Pressures up to 30 MPa. *J. Chem. Eng. Data* **1992**, *37*, 349−355.
(18) Oliveira, C. M. B. P.; Wakeham, W. A. The Viscosity of Five Liquid Hydrocarbons at Pressures Up to 250 MPa. *Int. J. Thermophys.* **1992**, *13*, 773−790.
(19) Dymond, J. H.; Awan, M. A.; Glen, N. F.; Isdale, J. D. Transport Properties of Nonelectrolyte Liquid Mixtures. VIII. Viscosity Coefficients for Toluene and for Three Mixtures of Toluene + Hexane from 25 to 100 °C at Pressures up to 500 MPa. *Int. J. Thermophys.* **1991**, 275−287.
(20) Assael, M. J.; Papadaki, M.; Wakeham, W. A. Measurements of the Viscosity of Benzene, Toluene, and *m*-Xylene at Pressure up to 80 MPa. *Int. J. Thermophys.* **1991**, *12*, 449−457.
(21) Vieira Dos Santos, F. J.; Nieto De Castro, C. A. Viscosity of Toluene and Benzene under High Pressure. *Int. J. Thermophys.* **1997**, *18*, 367−378.
(22) Stephan, K.; Lucas, K. *Viscosity of Dense Fluids*; Plenum Press: New York and London, 1979.
(23) Knapstad, B.; Skjolsvik, P. A.; Oye, H. A. Viscosity of Pure Hydrocarbons. *J. Chem. Eng. Data* **1989**, *34*, 37−43.
(24) Van Der Gulik, P. S. Viscosity of Carbon Dioxide in the Liquid Phase. *Physica A* **1997**, *238*, 81−112.
(25) Younglove, B. A.; Ely, J. F. Thermophysical Properties of Fluids. II. Methane, Ethane, Propane, Isobutane, and Normal Butane. *J. Phys. Chem. Ref. Data* **1987**, *16*, 577−798.

(26) Vogel, E.; Küchenmeister, C. Viscosity Surface Correlation of Propane. *High Temp.-High Pressure* **1997**, *29*, 397−404.
(27) CREPS Géopétrole, *Viscosité et Masse Volumique des Paraffines Légères, de l′Azote et du Dioxide de Carbone*; Editions Technip: Paris, 1970.
(28) Knapstad, B.; Skjolsvik, P. A.; Oye, H. A. Viscosity of *n*-Decane−Methane System in the Liquid Phase. *Ber. Bunsen-Ges. Phys. Chem.* **1990**, *94*, 1156−1165.
(29) Sage, B. H.; Berry, V. M. *Phase Equilibria in Hydrocarbon Systems: Behavior of the Methane−Propane−n-Decane System*; Monograph on API Research Project 37; American Petroleum Institute: 1971.
(30) Lee, B. I.; Kesler, M. G. A Generalized Thermodynamic Correlation Based on Three Parameters Corresponding States. *AIChE J.* **1975**, *21*, 510−527.
(31) Muñoz, F.; Reich, R. New Parameters for the LEE-KESLER Correlation Improve Liquid Density Prediction. *Fluid Phase Equilib.* **1983**, *13*, 171−178.
(32) Spencer, C. F.; Danner, R. P. Improved Equation for Prediction of Saturated Liquid Density. *J. Chem. Eng. Data* **1972**, *17*, 236−241.

Received for review December 6, 2000. Accepted March 7, 2001. This work has been accomplished within the European project EVIDENT under the JOULE Program, Contract No. JOF3-CT97-0034.

JE000371V